Low-temperature vibrational anharmonicity of ^{151}Eu in $EuBa_2Cu_3O_{7-\delta}$

1995 J. Phys.: Condens. Matter 7 2429

(http://iopscience.iop.org/0953-8984/7/12/007)

J. Phys.: Condens. Matter 7 (1995) 2429–2438. Printed in the UK

Low-temperature vibrational anharmonicity of ^{151}Eu in $EuBa_2Cu_3O_{7-\delta}$

M Capaccioli‡, L Cianchi†, F Del Giallo†, F Pieralli† and G Spina‡
† Istituto Ricerca Onde Elettromagnetiche, CNR, Firenze, Italy
‡ Dipartimento di Fisica, Università, Firenze, Italy

Received 9 November 1994

Abstract. The angular averaged mean-square displacement of ^{151}Eu in $EuBa_2Cu_3O_{7-\delta}$ was measured as a function of temperature by Mössbauer spectroscopy using the absorption area method. Large low-temperature anharmonicity was found; i.e. the adiabatic potential experienced by Eu^{3+} ions presents a 'wine-bottle bottom' shape with a flat region about 0.1 Å wide. Comparisons with other experimental results are made.

1. Introduction

Since the discovery of high-T_c superconductivity in cuprates, the contribution of phonons to the pairing has been debated, and it is a question not yet entirely understood [1]. In such a discussion, two features of cuprates must be considered: the ionic character of many bonds and the large amplitude of vibrational motions. The latter has been shown in many experiments.

Particular attention has been devoted to studing the apical oxygen vibrations and their effect in charge transfer between reservoirs and CuO_2 layers. EXAFS analysis seems to show the O(4) potential has a double-well shape with the two minima about 0.13 Å apart, along the c-axis direction [2]. Raman spectroscopy seems to confirm such a result [3]. Moreover, vibrational anomalies, such as low-temperature anharmonicity or anomalous behaviour around T_c, have been discovered by various techniques for other ions, such as Cu^{2+} [4], Ba^{2+} [5] and Eu^{3+} [6].

In a recent paper [7], anisotropic mean square displacement (MSD) of all atoms of $RBa_2Cu_3O_{7-\delta}$ (R = Ho, Y) were studied by neutron diffraction on single crystals. In contrast to EXAFS results, no strong anharmonic potential of the O(4) along c-axis was revealed, while anharmonic effects appeared in the ab planes. Moreover, it was shown that the Y and the ions of the CuO_2 planes are subjected to harmonic oscillations. Anharmonicities were drawn from these neutron experiments about the chain ions in the ab planes.

These results are in contrast to those obtained by Mössbauer spectroscopy of ^{151}Eu in $Eu_{1+x}Ba_{2-x}Cu_3O_{7-\delta}$ for $x = 0.15$, 0.25 where a strong low-temperature anharmonicity was shown for europium at the Y site [6], i.e. this ion experiences an adiabatic potential that presents a flat region. Since the flat region amplitude depends on x, it seems important to do a Mössbauer study of MSD of Eu in $EuBa_2Cu_3O_{7-\delta}$ ($x = 0$).

In this work, our aim is to obtain a very accurate value for MSD of Eu by Mössbauer spectroscopy in order to conclude this question. Actually, estimations of the Debye–Waller f factor of R^{3+} in RBCO (R = Eu, Gd) were already obtained using relative absorption area measurements (RAAM) [8]; however, this method is not reliable in the presence of

0953-8984/95/122429+10$19.50

low temperature anharmonicity [9]: the f values obtained from RAAM lead to absorption areas too great with respect to those observed. In fact, if the adiabatic potential of the Mössbauer ion does not have a parabolic, but a 'wine-bottle bottom' shape, for instance, (low-temperature anharmonicity), the ion oscillation amplitude will increase less (percentage wise) with the temperature than in a parabolic potential. In other words, in the presence of low-temperature anharmonicity, the ion MSD is greater than in the harmonic case and it is correlated not only to the Debye temperature but also to the amplitude of the potential flat region. This brings us to the conclusion that, if the MSD experimental data are fitted to a Debye model, the Debye temperature and f factor values will be overestimated. In order to avoid this, the absorption area method [9] will be used, which assures a very precise determination of the f value.

However, the Debye–Waller factor of ^{151}Sn in the Chevrèl phase $SnMo_6S_8$ was successfully determined by RAAM method and a large anharmonic contribution was found [10]. But here favourable conditions were met. First, the Mössbauer spectrum consists of a quadrupole doublet whose lines, due to Goldanski–Karyagin effect, have different intensities. From the ratio of the line intensities, the authors were able to determine the f factor components corresponding to oscillating motion parallel and perpendicular to γ-ray direction. Second, as their trend at high temperatures ($T > 80$ K) shows a smaller slope than at low temperatures, the authors concluded that the Sn vibrational motion displays large anharmonicity. The case is different for the isotope ^{151}Eu in EBCO; in fact, here we have an unresolved quadrupole structure and the spectrum consists of an enlarged single line, so the only information about the Debye–Waller factor comes from the absorption area. This also means that, as work is performed by powder sample, we can only obtain the angular average of the ion MSD.

In section 2, preparation of the samples and the experiment are described. In section 3 the method for the determination of the Debye–Waller factor from the absorption area of the spectra is briefly outlined. Finally, in section 4, the results found are reported and discussed.

2. Sample preparation and experiments

The material was prepared by the oxalate co-precipitation method [11] and was characterized by four probe resistometric measurements and by magnetic susceptibility. The critical temperature $T_c = 91$ K was obtained. The Mössbauer samples were prepared by mixing $EuBa_2Cu_3O_{7-\delta}$ powders with polythene powders, pressing them into holders made by an aluminum ring of 23 mm in diameter and two polythene dishes.

As we will see in the following, the absorption area method requires that we collect Mössbauer spectra of different thickness samples. So we prepared five samples containing 23.0, 44.2, 74.1, 104.0 and 141.6 mg cm^{-2} of EBCO. A SmF_3 source of 100 mCi was used at room temperature. For each sample, we collected spectra for eleven temperatures in the range 15–300 K. The cooling was obtained with a Gifford MacMahon cryogenerator and sample temperatures were stabilized within ± 0.1 K. Due to the very low counting rate (100 cs^{-1} for the thinnest sample), 3 days for collecting each spectrum were needed. Because of the spectra similarity, we only use the 15 K set as an example (figure 1).

In order to accurately determine the absorption area from one spectrum, we followed this procedure: let $N(v)$ be the *counting rates* corresponding respectively to Doppler velocity v and N_∞ the non resonant absorption counting rate ($v = \infty$). Further, let N_b be the counting

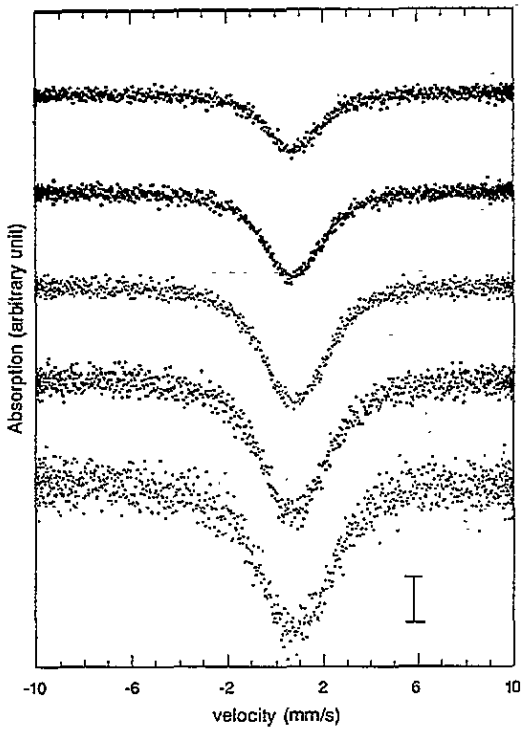

Figure 1. Absorption spectra obtained at $T = 15$ K for $EuBa_2Cu_3O_{7-\delta}$ samples, in order of growing thickness, starting from the top.

rate due to non Mössbauer photons (background radiation) then, posing

$$\varepsilon(v) = \frac{N_\infty - N(v)}{N_\infty - N_b} \tag{1}$$

the absorption area is given by

$$A = \int_{-\infty}^{+\infty} \varepsilon(v)\,\mathrm{d}v. \tag{2}$$

Due to thickness effects, the exact fitting function is generally very complex and it is consequently difficult to use in determining the absorption area A. In our case, because of electric quadrupole interaction, spectra are superpositions of a number of unresolved $2\Gamma_n$ linewidth Lorentzians having characteristic centres and intensities, apart from distortion induced by thickness effects. Since electric quadrupole interaction is small, the central part of spectra can be fitted well enough to Lorentzian doublet of the form

$$\frac{1}{2\pi}\frac{\Gamma_a}{(\Gamma_a/2)^2 + (v-\delta_1)^2} + \frac{1}{2\pi}\frac{\Gamma_a}{(\Gamma_a/2)^2 + (v-\delta_2)^2} \tag{3}$$

where Γ_a, δ_1 and δ_2 are fitting parameters. As thickness effects are greater near the maximum absorption, the wings of the experimental spectra will be not well fitted: in such a way an overestimation of N_∞ and, consequently, of A results [12].

At great distance from the centre, the spectrum will take on Lorentzian shape of linewidth $2\Gamma_n$ [13]. Therefore, in order to evaluate N_∞, we discarded the channels from each spectrum which correspond to an absorption greater than a suitable threshold. Then, each spectrum was fitted to Lorentzian doublet, having the form (3) with $2\Gamma_n$ substituting for Γ_a, assuming: (i) the number of discarded channels to be as small as possible; (ii) the fitted N_∞ almost independent of the threshold value. In our case a threshold $4.25\%N_\infty$ satisfies such criteria.

Concerning the N_b evaluation, we note that the SmF_3 source γ-ray spectrum consists of the Mössbauer transition sharp peak on a background as a result of other phenomena (mostly from the bremsstrahlung of the β^- emitted in the radioactive decay $^{151}Sm \rightarrow {}^{151}Eu$) (figures 2(*a*) and (*b*)). N_b is determined from the area of the region enclosed by the window of the single channel energy analyzer and by the interpolation of the background line inside this window (figure 2(*b*)). As the sample thickness influences the shape of the PHA energy spectrum, the N_b evaluation was performed for each sample.

A source of systematic error could arise from grain size effects. We note that their presence changes the absorption area of different thickness samples in different ways. This becomes evident considering a Mössbauer sample as a certain number of different sized grains randomly distributed in the sample volume. In order to determine the ℓ size grain contribution to the radiation absorption coefficient τ_{eff}, we imagine dividing the sample into layers with a thickness of ℓ. A photon can meet one grain or no grains crossing a single layer, then the probability for a photon to meet a certain number of grains is given by a binomial distribution. Taking this into account $\tau_{eff}(\ell)$ can be calculated for each ℓ. To obtain the contribution τ_{eff} of all grains the sum of all ℓ contributions must be determined. Denoting the absorption coefficient by $\bar{\tau}$ relative to a layer of homogeneous material with a thickness of $\sqrt[3]{\bar{v}}$, where $\bar{v}$ is the grain average volume, and by τ_0 that of a compact sample with mass m_t per unit area, the final result can be written in the form

$$\frac{\tau_{eff}-\tau_0}{\tau_0} = -\frac{1}{2}\bar{\tau}(\alpha_{10}-\alpha_{11}\,r) + \frac{1}{6}\bar{\tau}^2(\alpha_{20}-3\alpha_{21}\,r+2\alpha_{22}\,r^2)+\cdots \tag{4}$$

where $r = m_t/M$ is the ratio between the mass of the material and the mass that it would have, had it homogeneously filled the sample. Furthermore, α_{mn} are dimensionless quantities depending on the grain size distribution. Precisely

$$\alpha_{mn} = \frac{\sum_\ell \left(\dfrac{n(\ell)}{N_t}\right)^{m+n} \ell^{4m+3n}}{\bar{v}^{\frac{4}{3}m+n}} \tag{5}$$

where $n(\ell)$ and N_t are the number of ℓ size grains and the number of all grains respectively. Practically, the size grain distribution histogram is obtained from a granulometric analysis, so that $n(\ell)/N_t$ denotes the height of the ℓ centre bar.

We see the grain size effect brings about a systematic underestimation of the absorption coefficient and consequently of the absorption area. At the first order in $\bar{\tau}$ the absolute value of the absorption coefficient relative variation decreases linearly as a function of r, i.e. an increase of r leads to a perfect absorber.

3. Determination of the Debye–Waller factor

The Debye–Waller f factor was evaluated by the absorption area theoretical relation [9, 14]

$$A = f_s\frac{\pi t_a}{2}\frac{\Gamma_a}{\Gamma_n}e^{-t_a/2}\left[I_0(t_a/2)+I_1(t_a/2)\right] \tag{6}$$

where Γ_a is the linewidth of the ideal zero thickness sample, Γ_n the natural linewidth, $t_a = f_a n_a \sigma_0$ the dimensionless thickness of the absorber, and I_n is the nth order modified Bessel function. Furthermore f_a and f_s are the Debye–Waller factor of the absorber and source respectively, n_a the number of Mössbauer atoms per cm^2 and σ_0 is the resonant cross section. According to [15], f_s, at 300 K, was set to 0.485±0.005. In equation (6) the quantities Γ_a and t_a are temperature dependent parameters.

In order to find Γ_a at each temperature, the linewidth Γ of every spectrum was determined as a function of n_a. Then we considered the following empirical relation [16], which is valid for single line spectrum, neglecting the small instrumental line broadening

$$\Gamma(T, n_a) = \Gamma_s + \Gamma_a(T) + k(T)n_a. \tag{7}$$

From equation (7) we obtained the zero thickness intercept $\Gamma_s + \Gamma_a$ by linear best fits. In order to find Γ_s we performed Mössbauer spectra at 300 K on a set of different thickness samples of F_3Eu, which is the source material, so that here $\Gamma_s + \Gamma_a = 2\Gamma_s$. The linear best fit of the line-widths gave $\Gamma_s = 1.26 \pm 0.02$ mms^{-1} [12].

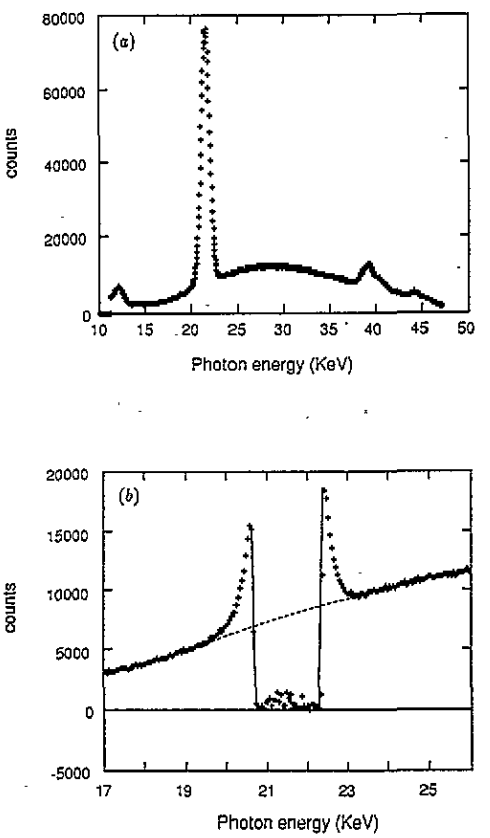

Figure 2. (*a*) PHA energy spectrum through the sample with 23.0 mg cm^{-2} of EBCO. The sharp 21.6 keV peak, which corresponds to the Mössbauer transition, rises from the background radiation. (*b*) Single channel analyzer window centred on the Mössbauer peak. The area of the region delimited from the single channel window and the dotted line gives N_b.

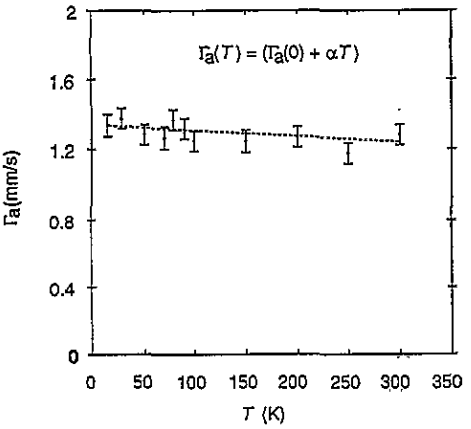

Figure 3. Γ_a values at the eleven considered temperatures. The dashed line represents the linear best fit.

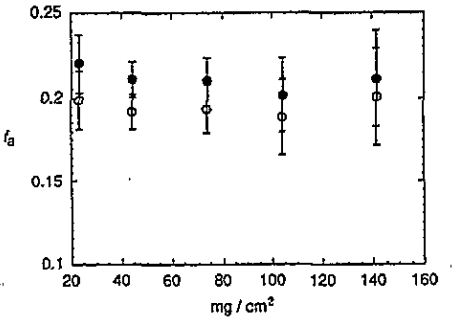

Figure 4. f_a values at $T = 300$ K for the five samples. Full circles denote corrected values taking into account the grain size effect and the empty ones denote not corrected values.

Figure 3 shows the Γ_a values obtained in the way described above as a function of T. As the differences among the $\Gamma_a(T)$ values are mainly attributed to random errors, such data were linearly fitted by the relation

$$\Gamma_a(T) = \Gamma_a(0) + \alpha T. \tag{8}$$

The values $\alpha = -0.0004 \pm 0.0002$ mm s^{-1} K^{-1} and $\Gamma_a(0) = 1.34 \pm 0.03$ mm s^{-1} were obtained. We note that by increasing the temperature from 0 to 300 K, Γ decreases about 9%. This can be attributed to a slight T dependence of the small quadrupole interaction.

Knowing f_s and $\Gamma_a(T)$, the $t_a(T)$ values and consequently those of $f_a(T)$ can be determined from the experimental absorption areas of the five samples by equation (6).

In order to estimate the grain size effect, a granulometric analysis of the powders was made by processing their optical microscope images. We obtained: $(\bar{v})^{1/3} \simeq 5\,\mu$m, $\bar{\tau} \simeq 0.12$, $\alpha_{10} \simeq 2.0$ and $\alpha_{11} \simeq 2.4$; consequently, since $M \simeq 300$ mg cm^{-2}, the correction to the absorption coefficient ranges from about 10% for the thinnest sample to about 5% for the thickest sample. Figure 4 shows, for instance, the obtained f_a values of the five samples at $T = 300$ K along with those corrected, taking the grain size effect into account. Therefore, the grain size effect corrections to f are of an order comparable to the accidental errors.

4. Results and conclusions

From the relation

$$f_a = \exp(-k^2\langle x^2\rangle_T) \tag{9}$$

the angular average of the MSD $\langle x^2\rangle_T$ can be obtained.

As is well known, if the Mössbauer ion experiences a quasi parabolic potential, the moderate and high temperature ($T > \Theta_{D/2\pi}$) MSD data can be represented by the equation

[9]

$$\langle x^2 \rangle = \frac{3\hbar^2}{k_B M \Theta_{-2}^2} T \left[1 + 2\epsilon_{-2} T + \left(\frac{\Theta_{-2}}{6T} \right)^2 \right] \tag{10}$$

where Θ_{-2} is such that the moment

$$\mu_{-2} = \frac{1}{3N} \sum_{k,j} (\omega_{k,j})^{-2}$$

of the solid is equal to the moment of a Debye solid with Debye temperature $\Theta_D = \Theta_{-2}$: $\mu_{-2} = \int_0^{\Omega_{-2}} \rho(\omega)\, \omega^{-2}\, d\omega$, where $\rho(\omega)$ is the Debye state density and $\Omega_{-2} = k_B \Theta_{-2}/\hbar$. Also ϵ_{-2} expresses the high-temperature anharmonic effects. We note that the quantity

$$Y = \langle x^2 \rangle - \frac{\hbar^2}{12 k_B M T} = \frac{3\hbar^2}{k_B M \Theta_{-2}^2} [T + 2\epsilon_{-2} T^2] \tag{11}$$

for quasi-parabolic potential (no low temperature anharmonicity) and for $T > \Theta_{D/2\pi}$, is represented by a parabola branch passing through the origin. As the Debye temperature Θ_D for EBCO is in the range 300–400 K, the previous relation is certainly valid for $T \geqslant 100$ K. If the potential shape is flat around the minimum (low-temperature anharmonicity), the parabola branch representing Y will be shifted by a positive quantity Y_0 which measures the order of magnitude of this flat region [17]. In figure 5 we display the obtained high temperature Y values for the five samples.

For each sample, Y can be fitted with a linear relation, which means the high temperature anharmonicity is negligible. Corresponding Y_0 values are provided from zero-temperature intercepts of the linear fits. We note that the Y_0 values obtained for the five samples agree with each other within the expected errors. Then we can conclude that the non zero value for Y_0 is not related to experimental effects, as grain size or dead time effects [18]. However, we are aware that, in order to make our results more convincing, further careful measurements should be performed on other europium compounds. Such measurements will be the subject matter of a following work. Here we can only mention data concerning some of our old Debye–Waller factor measurements of ^{151}Eu in Eu_2O_3 and EuF_3. Such measurements gave MSD values $\frac{1}{3} \div \frac{1}{2}$ of the EBCO value. This difference strongly indicates that our result about the anharmonicity in EBCO cannot be explained by systematic errors in the procedure used.

From our data, the amplitude of the potential flat region in EBCO results in the order of $\sqrt{Y_0} \simeq 0.1$ Å . This is also the order of magnitude of ^{151}Eu oscillation amplitude at low temperature. If we take into account the oscillation frequencies of the europium ion as they result from IR and Raman measurement [19] and we calculate the corresponding harmonic MSD, we obtain 0.02 Å for $T = 0$ K and 0.03 Å for $T = 300$ K.

The oscillation amplitude of the europium ion is then appreciably greater with respect to those of ordinary atomic potential, even at high temperatures.

Since we use powder samples, our MSD results should be a mean of the MSD in the c and ab plane directions. It can be observed that these results contrast with neutron diffraction values for MSD of the same site (figure 6). A similar contrast was found between EXAFS and the same neutron diffraction measurements at the O(4) site. The first of these techniques provides a double well potential for O(4) ions along the c-axis, while neutron diffraction provides an harmonic potential [2, 7].

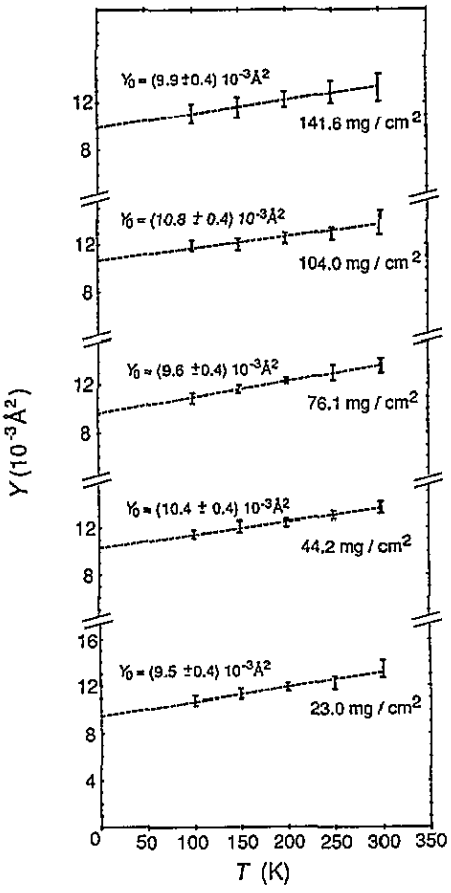

Figure 5. *Trend of Y against T for the five samples. Y_0 denotes zero-temperature intercept of data linear fit.*

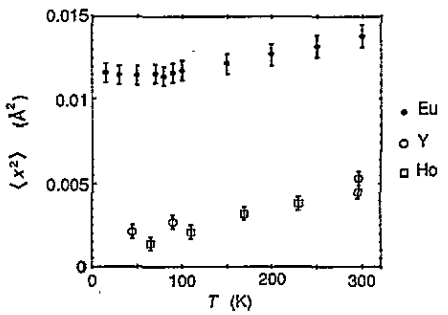

Figure 6. *MSD angular average against T for ^{151}Eu in* EBCO obtained by Mössbauer spectroscopy and for Y and Ho (in YBCO and HBCO respectively) obtained with neutron diffraction, adapted from [7].

Assuming that there are no experimental misunderstandings, we pose the following question: might mean square displacements obtained by Mössbauer spectroscopy or EXAFS, in some cases, differ from those obtained by neutron or X-ray diffraction?

Concerning this, we note that by Mössbauer spectroscopy the temporal average of the square displacement of an ion is measured and EXAFS information concerns the relative positions of an ion with respect to its nearest neighbour. Thus, local displacements are experienced in both cases. On the contrary, the MSD derived from neutron diffraction measures the relative position changes of ions lying on adjacent planes of the same Bravais sublattice. Therefore, if the motion of such ions were strongly correlated, it would be possible to have different results from local and not local averages of the square displacements.

Also, through comparison of the two averages, information about the vibrational motions of the crystal ions could be drawn. For instance, let us consider the two B_{1u} optical modes shown in figure 7 for ($k = 0$) [20]. In the mode of figure 7(a) the Eu^{3+} Bravais sublattice oscillates as a whole, so that it gives no contribution to the not local MSD measure, while

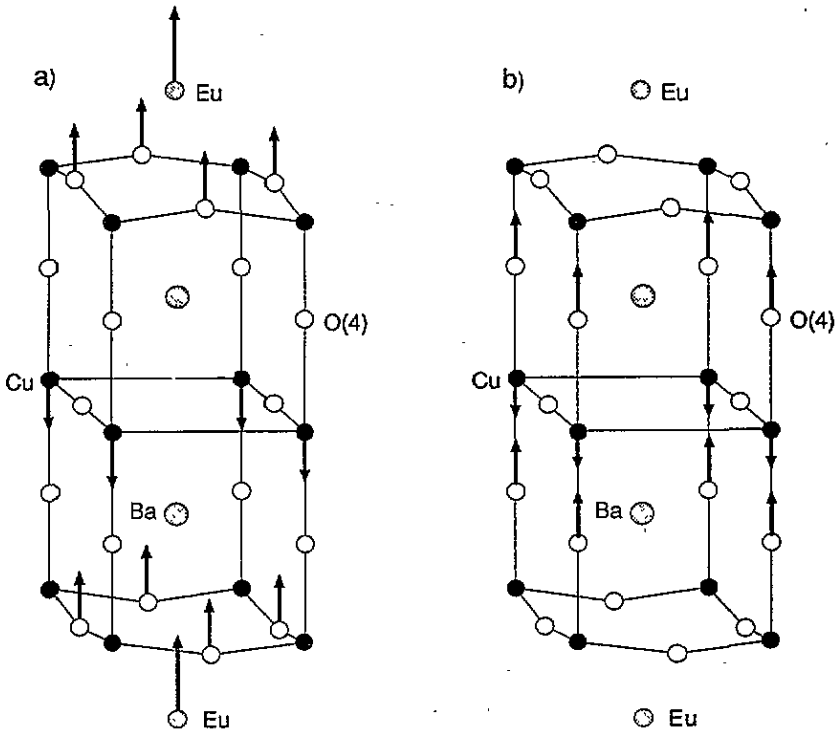

Figure 7. Normal mode displacement of symmetry B_{1u} involving (*a*) the motion of the Eu ions and (*b*) the motion of the O(4) ions.

it contributes to local MSD measure. Actually this is exactly true only for $k = 0$ or for small enough values of k. However the Eu^{3+} ion motions remain strongly correlated for all modes of the optical branch considered. Similar conclusions can be drawn for the O(4) ion motion concerning the optical branch of figure 7(*b*). Then, if the excitation energy of such optical branches was small enough and the corresponding motions displayed low-temperature anharmonicities, these anharmonicities could not be revealed through non local measurement. However, this is only a possible qualitative explanation, the final answer to the question requires further theoretical and experimental studies.

Acknowledgment

This work was partially supported by the National Research Council of Italy, CNR, under the Progetto finalizzato 'Superconductive and Cryogenic Technologies'.

References

[1] Pickett W E, Krakauer H, Cohen R E and Singh D J 1992 *Science* **255** 46
Anderson P W 1992 *Science* **256** 1526
[2] Mustre da Leon J, Conradson S D, Batistić I, Bishop A R, Raistrick I D, Aronson M C and Garzon F H 1990 *Phys. Rev. Lett.* **65** 1675; 1992 *Phys. Rev.* B **65** 2447
[3] Gasparov L V, Kulakovskiĭ V B , Timofeev V B and Sherman V Ya 1991 *Sov. Phys.–JETP* **73** 929

[4] Sharma R P, Rehn L E, Baldo P M and Liu J Z 1989 *Phys. Rev. Lett.* **62** 2869
Haga T, Yamaya K, Abe Y, Tajima Y and Hidaka Y 1990 *Phys. Rev.* B **41** 826
Rehn L E, Sharma R P, Baldo P M, Chang Y C and Jiang P Z 1990 *Phys. Rev.* B **42** 4175
Mook H A, Mostoller M, Harvey J A, Hill N W, Chakoumakos B C and Sales B C 1990 *Phys. Rev. Lett.* **65** 2712

[5] Marsh P, Siegrist T, Fleming R M, Schneemeyer L F and Waszczak J V 1988 *Phys. Rev.* B **38** 874
Sasaki S, Kawaguchi K and Nakao M 1992 *Japan J. Appl. Phys.* **31** L467

[6] Cianchi L, Del Giallo F, Pieralli F, Mancini M, Sciortino S, Spina G, Ammannati N and Garré R 1991 *Solid State Commun.* **80** 705

[7] Schweiss P, Reichardt W, Braden M, Collin G Heger G, Claus H and Erb A 1994 *Phys. Rev.* B **49** 1387

[8] Boolchand P, Enzweiler R N, Zitkovsky I, Meng R L, Hor P H, Chu C W and Huang C Y 1987 *Solid State Commun.* **63** 521
Bornemann H-J, Czjzek G, Ewert D, Meyer C and Renker B 1987 *J. Phys. F: Met Phys.* **17** L337
Wortmann G, Blumenröder S, Freimuth A and Riegel D 1988 *Phys. Lett.* **126A** 434

[9] Kolk B 1984 *Dynamical Properties of Solids* vol 5, ed G K Horton and A A Maradudin (Amsterdam: North Holland)

[10] Kimball C W, Weber L, Van Landuyt G, Fradin F Y, Dunlap B D and Shenoy G H 1976 *Phys. Rev. Lett.* **36** 412

[11] Ammannati N, Barani G, Garré R and Magnanelli S 1989 *Vuoto* **19** 24

[12] Capaccioli M, Cianchi L, Del Giallo F, Pieralli F, Moretti P and Spina G unpublished

[13] Janot C 1972 *L'effet Mössbauer et ses Applications a la Physique Solide (Paris)* p 76

[14] Abe N and Shwartz L H 1973 *Mössbauer Effect Methodology* vol 8, ed I J Gruverman and C W Seidel (New York: Plenum)

[15] Agresti D G, Belton M, Webb J and Long S 1974 *Mössbauer Effect Methodology* vol 9, ed I J Gruverman and C W Seidel (New York: Plenum)

[16] O'Connor D A 1963 *Nucl. Instrum. Methods* **21** 318

[17] Dash J G, Johnson D P and Visscher W M 1968 *Phys. Rev.* **168** 1087

[18] Love J C, Obenshain F E and Czjzek G 1971 *Phys. Rev.* B **3** 2827

[19] Thomsen C and Cardona M 1989 *Physical Properties of High Temperature Superconductors I* ed D M Ginsberg (Singapore: World Scientific) p409

[20] Cardona M 1992 *Proc. XXI Europ. Congress on Molecular Spectroscopy* p 211